



Published in final edited form as:

J Child Neurol. 2018 September ; 33(10): 642–650. doi:10.1177/0883073818776157.

Absence of Axoglial Paranodal Junctions in a Child With *CNTNAP1* Mutations, Hypomyelination, and Arthrogryposis

Alexander Conant, BA¹, Julian Curiel, BS², Amy Pizzino, MS¹, Parisa Sabetrasekh, MD¹, Jennifer Murphy, CPNP³, Miriam Bloom, MD⁴, Sarah H. Evans, MD⁵, Guy Helman, BS^{1,6,7}, Ryan J. Taft, PhD^{8,9}, Cas Simons, PhD^{7,9}, Matthew T. Whitehead, MD^{10,11}, Steven A. Moore, MD, PhD¹², Adeline Vanderver, MD^{1,2,3,11}

¹Department of Neurology, Children's National Health System, Washington, DC, USA

²Department of Neurology, Children's Hospital of Philadelphia, Philadelphia, PA, USA

³National Human Genome Research Institute, National Institutes of Health, Bethesda, MD, USA

⁴Department of Pediatric Hospitalist Medicine, Children's National Health System, Washington, DC, USA

⁵Department of Physical Medicine and Rehabilitation, Children's National Health System, Washington, DC, USA

⁶Center for Genetic Medicine, Children's National Health System, Washington DC, USA

⁷Murdoch Children's Research Institute, Parkville, Melbourne, Australia

⁸Illumina, San Diego, CA, USA

⁹Institute for Molecular Bioscience, University of Queensland, St. Lucia, Queensland, Australia

¹⁰Neuroradiology Department, Children's National Health System, Washington, DC, USA

¹¹George Washington University School of Medicine, Washington, DC, USA

¹²Department of Pathology, University of Iowa Carver College of Medicine and Paul D. Wellstone Muscular Dystrophy Cooperative Research Center, Iowa City, IA, USA

Abstract

Article reuse guidelines: sagepub.com/journals-permissions

Corresponding Authors: Adeline Vanderver, MD, Children's National Medical Center, Center for Genetic Medicine Research, 111 Michigan Ave NW, Washington, DC 2970, USA. avanderv@childrensnational.org, Steven A. Moore, MD, PhD, Department of Pathology, University of Iowa Carver College of Medicine and Paul D. Wellstone Muscular Dystrophy Cooperative Research Center, Iowa City, IA, USA. vandervera@email.chop.edu.

Author Contributions

Conceptualization: AV, RJT, CS, and SAM. Methodology, investigation, and validation: AC, AP, PS, CS, RJT, JM, MB, SHE, GH, MTW, SAM, and AV. Writing original draft: AC, JC, AP, PS, SAM, AV. Manuscript reviewing and editing: JC, JM, MB, SHE, GH, RJT, CS, MTW.

Declaration of Conflicting Interests

The authors declared no potential conflicts of interest with respect to the research, authorship, and/or publication of this article.

Ethical Approval

This study was approved by the IRB of Children's National and Children's Hospital of Philadelphia.

Leukodystrophies and genetic leukoencephalopathies are a heterogeneous group of heritable disorders that affect the glial-axonal unit. As more patients with unsolved leukodystrophies and genetic leukoencephalopathies undergo next generation sequencing, causative mutations in genes leading to central hypomyelination are being identified. Two such individuals presented with arthrogryposis multiplex congenita, congenital hypomyelinating neuropathy, and central hypomyelination with early respiratory failure. Whole exome sequencing identified biallelic mutations in the *CNTNAP1* gene: homozygous c.1163G>C (p.Arg388Pro) and compound heterozygous c.967T>C (p.Cys323Arg) and c.319C>T (p.Arg107*). Sural nerve and quadriceps muscle biopsies demonstrated progressive, severe onion bulb and axonal pathology. By ultrastructural evaluation, septate axoglial paranodal junctions were absent from nodes of Ranvier. Serial brain magnetic resonance images revealed hypomyelination, progressive atrophy, and reduced diffusion in the globus pallidus in both patients. These 2 families illustrate severe progressive peripheral demyelinating neuropathy due to the absence of septate paranodal junctions and central hypomyelination with neurodegeneration in *CNTNAP1*-associated arthrogryposis multiplex congenita.

Keywords

Boylan-Dew-Greco syndrome; lethal congenital contracture syndrome 7; hypomyelination; myelin; Caspr1; leukodystrophy; whole exome sequencing; pathology

Leukodystrophies and genetic leukoencephalopathies are a heterogeneous group of heritable disorders affecting the glial axonal unit in the nervous system, particularly the central nervous system white matter.^{1,2} Leukodystrophies affect approximately 1 in 7600 births³ and historically about 50% of individual cases remain unsolved.² For individuals presenting with myelin abnormalities affecting the central nervous system, a number of disorders are not canonical leukodystrophies, including disorders of protein translation, cytoskeleton, and mitochondrial function. As a growing number of individuals with unsolved leukodystrophies undergo next generation sequencing, causative mutations in genes not previously associated with central hypomyelination are being identified.⁴

A subset of heritable, severe, early onset myelin abnormalities affecting the peripheral nervous system are classified as congenital hypomyelinating neuropathies. These have previously been linked to defects in myelin related proteins⁵ and proteins associated with Schwann cell-basement membrane interactions.^{6,7} Arthrogryposis multiplex congenita is a severe phenotype seen in some cases of congenital hypomyelinating neuropathy. Arthrogryposis multiplex congenita is variously reported as affecting from 1 in 3000⁸ to 1 in 12 000⁹ live births. A large proportion of reported arthrogryposis multiplex congenita cases never achieved a molecular diagnosis¹⁰ or preceded the availability of genetic testing.¹⁰⁻¹⁶ Here, we describe 2 individuals with mutations in the *CNTNAP1* gene who were identified in a whole exome screen of individuals with unsolved leukodystrophies.⁴

The *CNTNAP1* gene encodes contactin-associated protein 1 (Caspr1). Caspr1 is a cell-adhesion protein tightly associated in *cis* with contactin in the paranodal axolemma; together they bind to the glial cell ligand, neurofascin 155 (NF155).¹⁷ In both the central nervous system and peripheral nervous system, these 3 proteins form the septate-like paranodal

junctions (aka transverse bands) between the axolemma and paranodal myelin sheath terminal loops. By separating the voltage-gated sodium channels from the delayed rectifier potassium channels in nodes of Ranvier and the juxtaparanodal region, respectively, this protein junctional complex plays a critical role in facilitating high-velocity nerve conduction and myelin homeostasis. Previously described families (n = 9) with *CNTNAPI* mutations (lethal congenital contracture syndrome 7-OMIM #616286)^{10,18–21} were found to have congenital hypomyelinating neuropathy with disease onset before birth, contractures in distal joints, motor paralysis, hypotonia, and polyhydramnios; death occurred within a few months of birth unless artificial ventilation was performed. Serial brain magnetic resonance imaging (MRI) evaluations of the 2 new patients reported here confirm that the disease phenotype of *CNTNAPI* mutations includes progressive leukodystrophy with brain volume loss.^{18,19} In addition, sural nerve and muscle biopsies in 1 of these individuals show dramatically progressive, sensorimotor neuropathy, and confirm the finding that *CNTNAPI* mutations result in the absence of septate axoglial paranodal junctions.^{18,21}

Methods

Patient Recruitment

Patients and their families were collected prospectively in the Myelin Disorders Bioregistry Project with approval from the institutional review board at Children's National Health System. Written informed consent was obtained for each study participant. Informed consent included consent for exome sequencing approaches and the risks and benefits were covered. Genomic DNA samples were collected from blood samples provided to the bioregistry.

Clinical Characterization

Patients were examined and characterized by AV. Clinically obtained MRIs were reviewed by MTW. All MRI exams were of diagnostic quality.

Skeletal Muscle and Peripheral Nerve Biopsies

Muscle biopsies were processed routinely for frozen and paraffin section light microscopic evaluation. This included standard histochemistry and enzyme histochemistry (hematoxylin-eosin stain, adenosine triphosphatase, reduced nicotinamide adenine dinucleotide, succinic dehydrogenase, and cytochrome oxidase [COX]) as well as immunoperoxidase staining of slow and fast myosin heavy chains. A small portion of muscle biopsy was also fixed in glutaraldehyde and processed into epon blocks for electron microscopy. Nerve biopsies were fixed in isomolar glutaraldehyde and processed into epon blocks for electron microscopy. The control sural nerve used to demonstrate normal septate axoglial paranodal junctions in Figure 4C was surgically removed from a 45-year-old woman to relieve otherwise intractable pain secondary to a remote ankle fracture.

Exome Sequencing and Analysis

Whole exome sequencing was performed on all affected individuals and their parents.¹⁰ Sequencing was performed at the Queensland Centre for Medical Genomics. Subsequent analysis and identification of candidate variants was performed with an in-house workflow incorporating the annotated variant data and pedigree information.

Results

Patient Identification

Within our bioregistry patient population, 2 patients were identified with similar clinical manifestations of congenital hypomyelinating neuropathy, early respiratory insufficiency, and arthrogryposis multiplex congenita. Both individuals were found to harbor potentially pathogenic variants in *CNTNAPI* (Figures 1A and 1B) and were previously published as part of a larger cohort.⁴ Parents, although obligate heterozygotes, were not assessed as part of this study.

Sequencing Results

LD_0158.0 was homozygous for c.1163G>C (p.Arg388Pro) variant, which has been previously found in another infant²² and LD_0333.0 was a compound heterozygote with c.967T>C (p.Cys323Arg), a pathogenic finding previously reported,^{20,21} and c.319C>T (p.Arg107*) variants (Figures 1A and 1B). p.Arg388Pro and p.Cys323Arg are predicted as likely pathogenic^{20–23} by SIFT and PolyPhen and are both conserved in all vertebrates back to fish. p.Cys323Arg is responsible for forming a disulfide bond to C355. Both of these variants are in or near laminin-G like domains (Figure 1B), which are thought to play a role in interacting with receptors or ligands.²⁴ The c.319C>T (p.Arg107*) variant causing early termination is classified as pathogenic.

Clinical Characterizations

Individual LD_0158.0 is an 8 year old male with hypotonia and respiratory failure requiring intubation at birth and subsequent tracheotomy-dependency, congenital hypomyelinating neuropathy with arthrogryposis multiplex congenita, cleft palate, cortical vision loss, bilateral hearing loss, and neurogenic bladder. His birth history is significant for polyhydramnios. He had an older brother with a similar phenotype who died at 48 hours of age due to respiratory distress. Nerve conduction studies and electromyography (EMG) at 3 weeks of age showed prolongation of distal latencies and slow nerve conduction velocity (11.1 m/s at distal median) with decreased motor unit recruitment suggestive of a neurogenic disorder with features consistent with a demyelinating peripheral neuropathy. At age 8 years, he is maintained on artificial ventilation, with very limited developmental outcomes and no independent motor skills, hypotonia with hyporeflexia, and seizures controlled with topiramate. Assessment of cognitive developmental outcomes is limited by the severe motor disability seen in this individual.

Individual LD_0333.0 was a girl with severe hypotonia and respiratory insufficiency that required a tracheostomy after birth, hypomyelinating neuropathy, bilateral hearing loss, bilateral optic nerve atrophy, lethargy, and neurogenic bladder. She died at 8 years 3 months of pulmonary complications. Her birth history is significant for polyhydramnios. She had a younger sister with the same features who died soon after birth, and 2 unaffected older brothers.

MRI Features

LD_0158.0.—Brain MR performed at 4 days, 31 days, and 15 months demonstrated arrest of myelination, with most conspicuous hypomyelination at 15 months. The vermis was mildly hypoplastic. Brain volume evolved from normal to moderately decreased in the cerebrum and brainstem. Globi pallidi were initially abnormal in signal on T1WI and proton density images, and later demonstrated reduced diffusion at 15 months. Symmetric blunting of the limbus and shallow anterior segments were present in both ocular globes (Figure 1C).

LD_0333.0.—Neonatal brain MR at 11 days showed mild cerebral white matter volume loss, mild vermian hypoplasia, and abnormal globi pallidi proton density and T2 FLAIR signal but age-appropriate myelination. However, arrested myelination was present by 6 months and hypomyelination persisted at 15 months. Cerebral brain volume loss progressed from mild to severe. Ultimately, marked brainstem and moderate cerebellar volume loss also developed. Reduced diffusion in the globi pallidi, subthalamic nuclei, red nuclei, and superior cerebellar peduncles and decussations developed and increased in degree from 6 to 15 months. Symmetric blunting of the limbus and shallow anterior segments were present in both ocular globes. Single voxel magnetic resonance spectroscopy performed over the left parietal corticomedullary junction revealed elevated glutamine/glutamate, and mildly increased lipids and possibly lactate (Figure 1C).

Pathology Results

Biopsy results were available for LD_0158. A right quadriceps biopsy at 1 month of age showed mild atrophy of scattered muscle fibers without evidence of inflammation, myonecrosis, regeneration, or structural abnormalities (Figure 2). The fiber type distribution appeared normal (Figure 2A). A second muscle biopsy from the left quadriceps at 3.5 years demonstrated abnormal variation in fiber size with a marked type II fiber predominance and severe atrophy of type I fibers mimicking congenital myopathic disease (Figures 2B, 2C, and 2D).

His initial sural nerve biopsy (right sural) at 1 month of age showed a mildly reduced number of myelinated axons (Figure 3A). The myelinated axons present in the biopsy had a mild degree of abnormally thin myelin sheaths (Figures 3D and 3G). In addition, there were small onion bulbs, redundant basement membranes wrapping around empty Schwann cells (bands of Bungner), and some axons with dystrophic features. A second sural nerve biopsy (left sural) at 3.5 years of age showed severe demyelination and axonal pathology. The predominant pathology was axonal loss (Figure 3B). The few remaining myelinated axons were present within onion bulbs (Figure 3E). Many bands of Bungner were present (Figure 3H). In combination with the muscle biopsy at 3.5 years, there was evidence of sensory and motor neuropathy. Intramuscular nerve twigs were significant for axonal loss, axonal dystrophic changes, and de/remyelination with advanced onion bulb formation (Figures 3C, 3F, and 3I).

Schwann cell microvilli were sparse and blunted in each of the 3 nodes of Ranvier evaluated in longitudinal sections from the sural nerve biopsy at 3.5 years (Figures 4A and 4B). Abnormally broad Schwann cell processes formed the shoulders of each node. Terminal

loops of myelin were easily identified in the paranodal regions. Many had uniform shapes, and adherens junctions²⁵ were observed between some of the adjacent terminal loops. In some heminodes, abnormally shaped terminal loops were present immediately adjacent to the nodal region (Figure 4B). Remarkably, no septate-like axoglial paranodal junctions (aka transverse bands) were observed (Figure 4D).

Discussion

Peripheral myelination does occur despite mutations in *CNTNAPI* as demonstrated by published ultrastructural studies from the 32 and 36 gestational week sciatic nerves and the sural nerve biopsies in our patient at 1 month of age. Myelin also formed in mice with mutant *CNTNAPI*.^{24,26} Surprisingly, mutant mice had no discernable differences in sciatic nerve myelin thickness or axonal density, while all patients evaluated to date had early onset peripheral hypomyelinating neuropathy with thinning of the myelin sheath^{10,18,20–22} (Figure 3). Furthermore, the sensorimotor neuropathy in 1 of our patients progressed to near absence of myelinated axons and advanced onion bulb formation by 3.5 years of age.

Mutant mice lacking the Caspr/contactin complex do not have paranodal junctions.^{24,26,27} Potassium channels mislocalize to the paranodal region in both central nervous system and peripheral nervous system and peripheral nerve conduction velocities are substantially reduced. Although Na⁺ and K⁺ channel localization could not be evaluated in the biopsy tissue from our *CNTNAPI* patient, ultrastructural studies revealed nodal abnormalities strikingly similar to those of Caspr1 (NCP1) null mice²⁴ and shambler mice (*shm*) harboring homozygous *CNTNAPI* truncation mutations.^{18,21,26}

Central nervous system myelin involvement is also present in individuals affected by *CNTNAPI* mutations. Serial brain MRI evaluation of our patients demonstrated diffuse hypomyelination, progressive brain atrophy ranging from mild to severe, and reduced diffusion in globus pallidus with or without concurrent diffusion abnormalities in some white matter tracts of the brainstem and cerebellum. It should be noted that cerebellar atrophy has been reported in 3 different families^{18,19} as well as in 2 different mouse mutants relevant to *CNTNAPI*, NCP1^{-/-} mice²⁸ and *shm* mice.²⁹ It is possible that this atrophy is a reflection of neuronal loss (cell bodies and axons) in addition to alterations in myelin sheaths centrally. Most previously described individuals with arthrogryposis multiplex congenita and *CNTNAPI* mutations, died within the first few months of birth.^{10,18,19} Not surprisingly in view of the clinical severity of these presentations and the limitations of detecting myelin development by MRI in the first months of life, there is a lack of data on their central nervous system myelin pathology. More recently, MRIs in 2 long-term surviving children suggested persistent lack of myelination¹⁸ as seen in our affected individuals.

A second Caspr protein, Caspr2, functions to localize Kv1 potassium channels to the juxtaparanodal regions of the central nervous system and peripheral nervous system. Studies in mutant mice suggest that Caspr1 and Caspr2 are together critical for the proper localization of Kv1 channels.³⁰ A series of individuals with mild to moderate intellectual disability, seizures, hyporeflexia, and variable cortical dysplasia have been found to harbor

biallelic *CNTNAP2* mutations.^{31–37} Individuals with the milder intellectual disability phenotype seen with *CNTNAP2* mutations are also reported to have cerebellar atrophy and nonspecific multifocal T2 hyperintense white matter abnormalities.³⁷ It should be noted that although peripheral nerve pathology was not directly described in the milder intellectual disability phenotype seen with *CNTNAP2* mutations, a large number of these patients are noted to have hyporeflexia suggestive of underlying peripheral nerve abnormalities.³⁷

The absence of septate junctions resulting from *CNTNAPI* mutations may also explain the seizure phenotype seen in the longest living of our patients, as well as other patients harboring a similar phenotype resulting from *CNTNAPI* mutations.²¹ The Caspr/contactin complex is necessary to maintain voltage gated potassium channels (VGKC) in the juxtaparanodal region. Mutations in VGKC subunits and antibodies against the VGKC are known to result in seizures. It should be noted that epilepsy is a well-recognized phenotype in *CNTNAP2* mutations.^{31,35,37} Recently, autoantibodies to Caspr2 were hypothesized to result in an autoimmune encephalitis with seizures.³⁸ Mutant mice lacking the Caspr/contactin complex do not have central or peripheral paranodal junctions,^{24,26,27} and potassium channels mislocalize to the paranodal region in both locations. Although it is unknown at this point whether abnormalities would be seen in the human central nervous system, ultrastructural studies in 1 of our patients clearly demonstrated the absence of peripheral paranodal junctions as previously identified in individuals with *CNTNAPI* mutations.^{18,21} Murine models strongly suggest that nodal abnormalities are likely to also be present throughout the nervous system in humans. This has been demonstrated in humans with biallelic mutations to *GLDN*, encoding Gliomedin. Mutations to *GLDN* lead to a similar clinical spectrum as mutations to *CTNAPI*; however, expression of Gliomedin is limited to the peripheral nervous system whereas Caspr1 is expressed both in the peripheral nervous system and central nervous system. These patients show similar nodal pathology to *CNTNAPI* in the peripheral nervous system, providing evidence for a distinct disease group known as inherited nodopathies within the larger class of peripheral neuropathies.³⁹

Our report increases the number of individuals with congenital peripheral nerve hypomyelination/arthrogryposis multiplex congenita with *CNTNAPI* mutations, confirming that a range of phenotypes can be associated with these mutations. It is likely that the presentations of arthrogryposis multiplex congenita/hypomyelination and intellectual disability/epilepsy in individuals with *CNTNAPI* mutations represents a spectrum of disease manifestations that are the result of altered glial-axonal interactions and nodal electrophysiologic abnormalities. In the past, pediatric neurodegenerative conditions have been classified based on affected cell type. Leukodystrophies are thought to represent glial specific pathology, exemplified by hypomyelinating conditions such as Pelizaeus Merzbacher disease, which is caused by mutations in the oligodendrocyte specific gene *PLP1*.⁴⁰ *CNTNAPI* related disorders are neither a primary neuronal nor primary glial cell pathologic process, exemplifying the complex interactions between glial cells and neurons that may result in altered myelination and cellular electrophysiology.

Acknowledgments

We thank patients and their families.

Funding

The authors disclosed receipt of the following financial support for the research, authorship, and/or publication of this article: AP, GH, AC, and AV are supported by the Myelin Disorders Bioregistry Project. GH was supported by the Delman Fund for Pediatric Neurology Education. SAM is supported by U54-NS053672 that funds the Iowa, Paul D. Wellstone Muscular Dystrophy Cooperative Research Center.

References

1. Pizzino A, Pierson TM, Guo Y, et al. TUBB4A de novo mutations cause isolated hypomyelination. *Neurology*. 2014;83(10): 898–902. [PubMed: 25085639]
2. Vanderver A, Prust M, Tonduti D, et al. Case definition and classification of leukodystrophies and leukoencephalopathies. *Mol Genet Metab*. 2015;114(4):494–500. [PubMed: 25649058]
3. Bonkowsky J, Nelson C, Kingston J, Filloux F, Mundorff M, Srivastava R. The burden of inherited leukodystrophies in children. *Neurology*. 2010;75(8):718–725. [PubMed: 20660364]
4. Vanderver A, Simons C, Helman G, et al. Whole exome sequencing in patients with white matter abnormalities. *Ann Neurol*. 2016;79(6):1031–1037. [PubMed: 27159321]
5. Yonekawa T, Komaki H, Saito Y, Takashima H, Sasaki M. Congenital hypomyelinating neuropathy attributable to a de novo p. Asp61Asn mutation of the myelin protein zero gene. *Pediatr Neurol*. 2013;48(1):59–62. [PubMed: 23290023]
6. Boerkoel CF, Takashima H, Stankiewicz P, et al. Periaxin mutations cause recessive Dejerine-Sottas neuropathy. *Am J Hum Genet*. 2001;68(2):325–333. [PubMed: 11133365]
7. Baets J, Deconinck T, De Vriendt E, et al. Genetic spectrum of hereditary neuropathies with onset in the first year of life. *Brain*. 2011;134(pt 9):2664–2676. [PubMed: 21840889]
8. Richards S, Aziz N, Bale S, et al. Standards and guidelines for the interpretation of sequence variants: a joint consensus recommendation of the American College of Medical Genetics and Genomics and the Association for Molecular Pathology. *Genet Med*. 2015;17(5):405–424. [PubMed: 25741868]
9. Timpl R, Tisi D, Talts JF, Andac Z, Sasaki T, Hohenester E. Structure and function of laminin LG modules. *Matrix Biol*. 2000;19(4):309–317. [PubMed: 10963991]
10. Laquérière A, Maluenda J, Camus A, et al. Mutations in CNTNAP1 and ADCY6 are responsible for severe arthrogryposis multiplex congenita with axoglial defects. *Hum Mol Genet*. 2014; 23(9): 2279–2289. [PubMed: 24319099]
11. Hoff JM, Loane M, Gilhus NE, Rasmussen S, Daltveit AK. Arthrogryposis multiplexa congenita: an epidemiologic study of nearly 9 million births in 24 EUROCAT registers. *Eur J Obstet Gynecol Reprod Biol*. 2011;159(2):347–350. [PubMed: 22005589]
12. Boylan KB, Ferriero DM, Greco CM, Sheldon R, Dew M. Congenital hypomyelination neuropathy with arthrogryposis multiplex congenita. *Ann Neurol*. 1992;31(3):337–340. [PubMed: 1637141]
13. Charnas L, Trapp B, Griffin J. Congenital absence of peripheral myelin Abnormal Schwann cell development causes lethal arthrogryposis multiplex congenita. *Neurology*. 1988;38(6):966–966. [PubMed: 2835709]
14. Hakamada S, Kumagai T, Hara K, Miyazaki S, Miyazaki K, Watanabe K. Congenital hypomyelination neuropathy in a newborn. *Neuropediatrics*. 1983;14(3):182–183. [PubMed: 6312355]
15. Seitz R, Wechsler W, Mosny D, Lenard H. Hypomyelination neuropathy in a female newborn presenting as arthrogryposis multiplex congenita. *Neuropediatrics*. 1986;17(3):132–136. [PubMed: 3762869]
16. Pendlebury W, Berg K, Waters B, Emery E. Congenital hypomyelination neuropathy (CHN) associated with lethal arthrogryposis multiplex congenita (AMC): 187. *J Neuropathol Exp Neurol*. 1995;54(3):458.
17. Salzer JL. Polarized domains of myelinated axons. *Neuron*. 2003; 40(2):297–318. [PubMed: 14556710]
18. Hengel H, Magee A, Mahanjan M, et al. CNTNAP1 mutations cause CNS hypomyelination and neuropathy with or without arthrogryposis. *Neurol Genet*. 2017;3(2): e144. [PubMed: 28374019]

19. Lakhani S, Doan R, Almureikhi M, et al. Identification of a novel CNTNAP1 mutation causing arthrogryposis multiplex congenita with cerebral and cerebellar atrophy. *Eur J Med Genet.* 2017; 60(5):245–249. [PubMed: 28254648]
20. Nizon M, Cogne B, Vallat JM, et al. Two novel variants in CNTNAP1 in two siblings presenting with congenital hypotonia and hypomyelinating neuropathy. *Eur J Hum Genet.* 2016;25(1):150–152. [PubMed: 27782105]
21. Vallat JM, Nizon M, Magee A, et al. Contactin-associated protein 1 (CNTNAP1) mutations induce characteristic lesions of the paranodal region. *J Neuropathol Exp Neurol.* 2016;75(12):1155–1159. [PubMed: 27818385]
22. Mehta P, Kuspert M, Bale T, et al. Novel mutation in CNTNAP1 results in congenital hypomyelinating neuropathy. *Muscle Nerve.* 2017;55(5):761–765. [PubMed: 27668699]
23. Wu Z-Q, Li D, Huang Y, et al. Caspr controls the temporal specification of neural progenitor cells through notch signaling in the developing mouse cerebral cortex. *Cerebral Cortex.* 2017;27(2): 1369–1385. [PubMed: 26740489]
24. Bhat MA, Rios JC, Lu Y, et al. Axon-glia interactions and the domain organization of myelinated axons requires neurexin IV/Caspr/Paranodin. *Neuron.* 2001;30(2):369–383. [PubMed: 11395000]
25. Miyamoto T, Morita K, Takemoto D, et al. Tight junctions in Schwann cells of peripheral myelinated axons: a lesson from claudin-19-deficient mice. *J Cell Biol.* 2005;169(3):527–538. [PubMed: 15883201]
26. Sun XY, Takagishi Y, Okabe E, et al. A novel Caspr mutation causes the shambling mouse phenotype by disrupting axoglial interactions of myelinated nerves. *J Neuropathol Exp Neurol.* 2009;68(11):1207–1218. [PubMed: 19816196]
27. Boyle ME, Berglund EO, Murai KK, Weber L, Peles E, Ranscht B. Contactin orchestrates assembly of the septate-like junctions at the paranode in myelinated peripheral nerve. *Neuron.* 2001;30(2): 385–397. [PubMed: 11395001]
28. Garcia-Fresco GP, Sousa AD, Pillai AM, et al. Disruption of axoglial junctions causes cytoskeletal disorganization and degeneration of Purkinje neuron axons. *Proc Natl Acad Sci USA.* 2006; 103(13):5137–5142. [PubMed: 16551741]
29. Takagishi Y, Katanosaka K, Mizoguchi H, Murata Y: Disrupted axon-glia interactions at the paranode in myelinated nerves cause axonal degeneration and neuronal cell death in the aged Caspr mutant mouse shambling. *Neurobiol Aging.* 2016;43: 34–46. [PubMed: 27255813]
30. Gordon A, Adamsky K, Vainshtein A, et al. Caspr and caspr2 are required for both radial and longitudinal organization of myelinated axons. *J Neurosci.* 2014;34(45):14820–14826. [PubMed: 25378149]
31. Strauss KA, Puffenberger EG, Huettelman MJ, et al. Recessive symptomatic focal epilepsy and mutant contactin-associated protein-like 2. *N Engl J Med.* 2006;354(13):1370–1377. [PubMed: 16571880]
32. Jackman C, Horn ND, Molleston JP, Sokol DK. Gene associated with seizures, autism, and hepatomegaly in an Amish girl. *Pediatr Neurol.* 2009;40(4):310–313. [PubMed: 19302947]
33. Zweier C, de Jong EK, Zweier M, et al. CNTNAP2 and NRXN1 are mutated in autosomal-recessive Pitt-Hopkins-like mental retardation and determine the level of a common synaptic protein in *Drosophila*. *Am J Hum Genet.* 2009;85(5):655–666. [PubMed: 19896112]
34. Watson CM, Crinnion LA, Tzika A, et al. Diagnostic whole genome sequencing and split-read mapping for nucleotide resolution breakpoint identification in CNTNAP2 deficiency syndrome. *Am J Med Genet A.* 2014;164A(10):2649–2655. [PubMed: 25045150]
35. Rodenas-Cuadrado P, Pietrafusa N, Francavilla T, La Neve A, Striano P, Vernes SC. Characterisation of CASPR2 deficiency disorder—a syndrome involving autism, epilepsy and language impairment. *BMC Med Genet.* 2016;17:8. [PubMed: 26843181]
36. Zweier C. Severe intellectual disability associated with recessive defects in CNTNAP2 and NRXN1. *Mol Syndromol.* 2012;2(3–5): 181–185. [PubMed: 22670139]
37. Smogavec M, Cleall A, Hoyer J, et al. Eight further individuals with intellectual disability and epilepsy carrying bi-allelic CNTNAP2 aberrations allow delineation of the mutational and phenotypic spectrum. *J Med Genet.* 2016;53(12):820–827. [PubMed: 27439707]

38. Sunwoo JS, Lee ST, Byun JI, et al. Clinical manifestations of patients with CASPR2 antibodies. *J Neuroimmunol.* 2015;281:17–22. [PubMed: 25867463]
39. Maluenda J, Manso C, Quevarec L, et al. Mutations in GLDN, encoding gliomedin, a critical component of the nodes of ranvier, are responsible for lethal arthrogyriposis. *Am J Hum Genet.* 2016; 99(4):928–933. [PubMed: 27616481]
40. Fahim S, Riordan JR. Lipophilin (PLP) gene in X-linked myelin disorders. *J Neurosci Res.* 1986;16(1):303–310. [PubMed: 3746948]
41. Salman MS, Marles SL, Booth FA, Del Bigio MR. Early-onset neurodegenerative disease of the cerebellum and motor axons. *Pediatr Neurol.* 2009;40(5):365–370. [PubMed: 19380073]

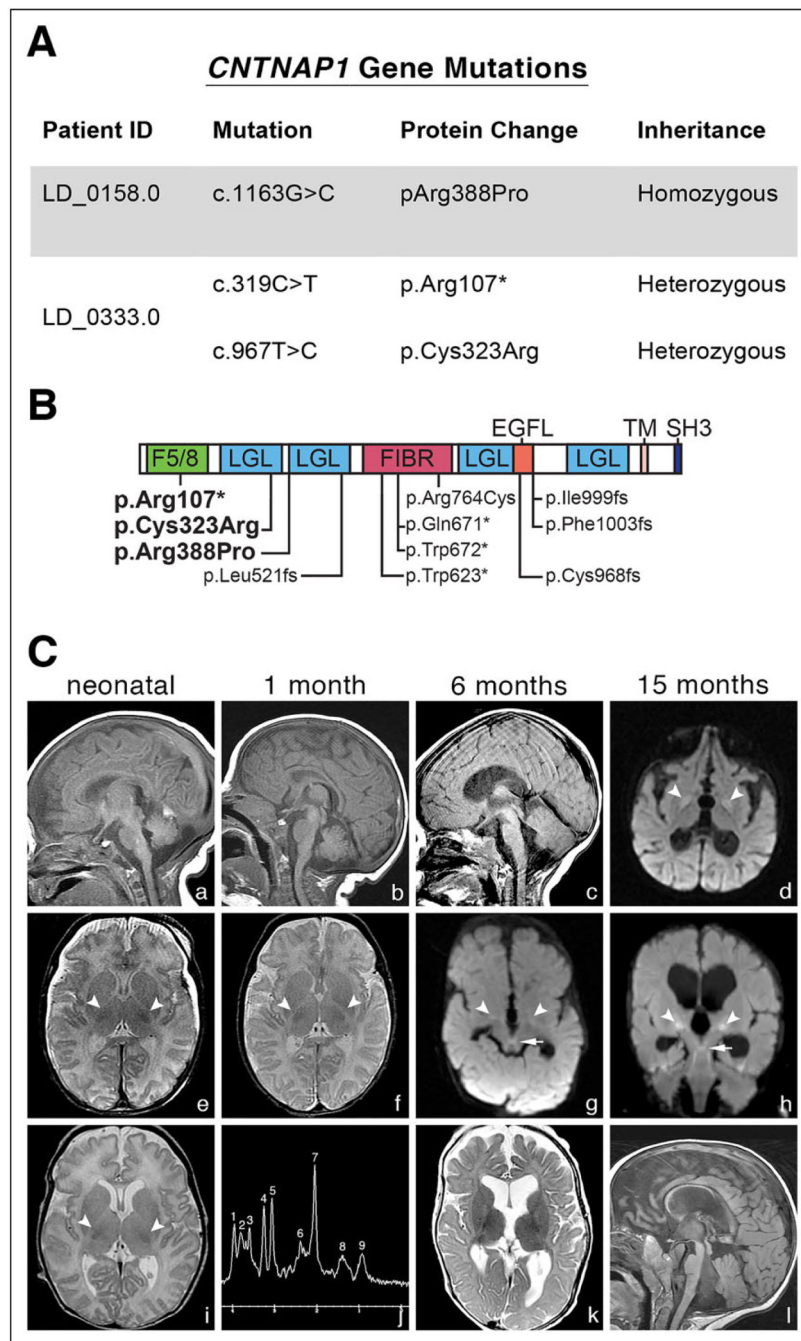


Figure 1. Genetic findings and neuroimaging in affected individuals. (A) *CNTNAP1* mutations in affected individuals. Whole exome sequencing revealed mutations predicted to be likely pathogenic⁴¹ in both patients. (B) Schematic of Caspr1 (encoded by *CNTNAP1*) showing the positions of pathogenic variants relative to predicted protein domains. Variants identified in this study are indicated in bold; previously identified variants unbolded.¹⁰ F5/8, F5/8 type C domain; LGL, Laminin G-like domain; FIBR, Fibrinogen C-terminal; EGFL, EGF-like domain; TM, Transmembrane; SH3, SH3-binding motif. (c) MRI imaging in *CNTNAP1*

mutated individuals. Multiple MR images from LD_0158.0 (a, b, d–f) and LD_0333.0 (c, g–l) performed in the 1st week of life (column 1), at 1 month (column 2), 6 months (column 3), and 15 months (column 4). Delayed myelination was present at birth on T2-weighted images in LD_0158.0 (e), with inconspicuity of the normally visible hypointense posterior limb internal capsule (PLIC) signal, in contrast to the normal T2WI from LD_0333.0 (i; arrows = PLIC). Delayed myelination was evident by 6 months in LD_0333.0 (k). Sagittal T1WI (a–c, l) and axial T2WI (f and k) show progressive brain atrophy in both CNTNAP1 patients. By 15 months, the cerebrum and brainstem showed marked volume loss with continued lack of myelination consistent with hypomyelination in LD_0333.0 (l). Both patients also developed reduced diffusion in the globi pallidi (d, g, h; large arrows). LD_0333.0 also had reduced diffusion in the superior cerebellar peduncles and decussations (g and h; small arrows), subthalamic nuclei, and red nuclei. Single voxel magnetic resonance spectroscopy (MRS) performed over the left parietal corticomedullary junction in LD_0333.0 (j) revealed elevated glutamine/glutamate, mildly increased lipids, and possibly lactate. MRS peaks correspond to Cr (creatine) = 1, Glx (glutamine and glutamate) = 2, MI (myoinositol) = 3, Cho (choline) = 4, Cr (creatine) = 5, Glx (glutamine and glutamate) = 6, NAA (N-acetylaspartate) = 7, lipid + lactate = 8, lipid = 9.

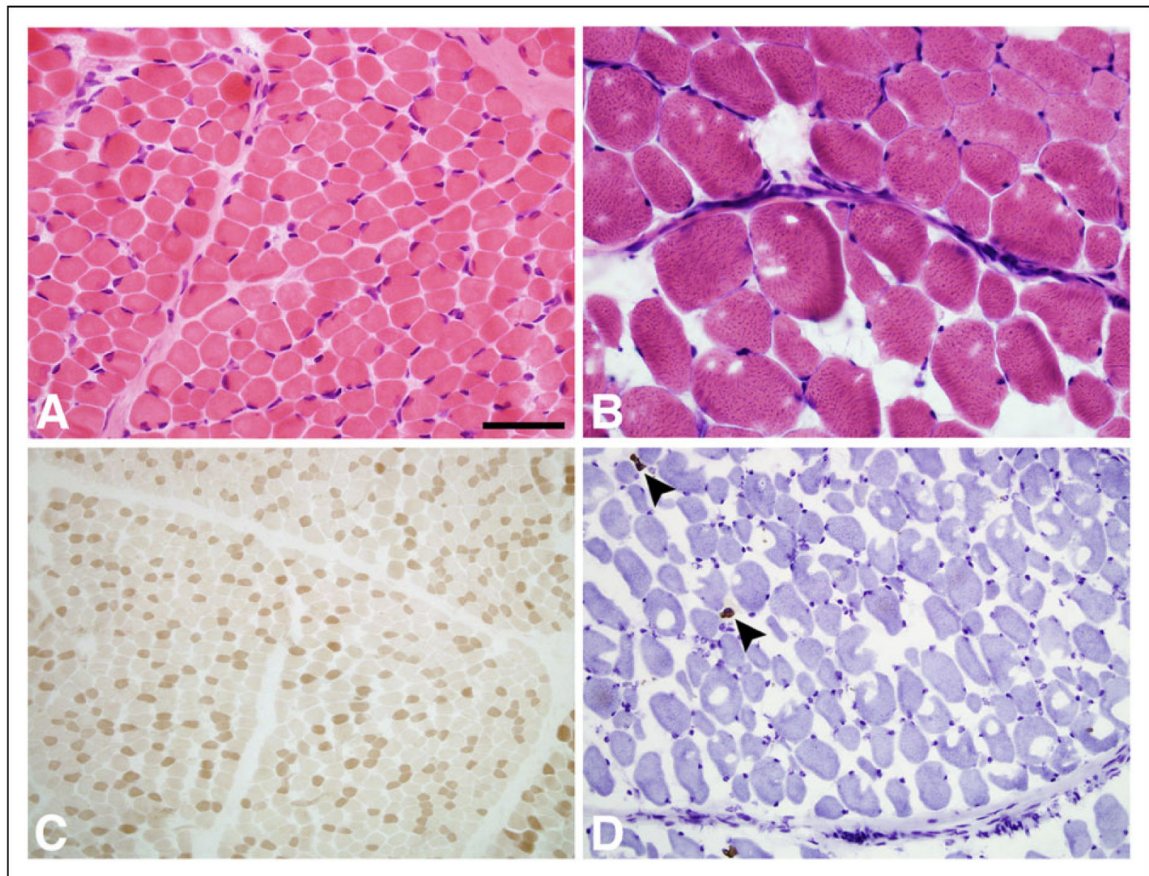


Figure 2. Muscle biopsy pathology in *CNTNAP1* mutated individuals. Panels A and B (hematoxylin-eosin stain) show mild variation in muscle fiber size at 1 month (A) and much greater variation in fiber size at 3.5 years (B) of age. Additional stains with adenosine triphosphatase pH 4.3 (C) and slow myosin immunoperoxidase (D) show the fiber type distribution. At 1 month, the fiber type distribution is normal. At 3.5 years of age, there are only rare type I fibers (arrowheads); these type I fibers are extremely atrophic. The size bar is 100 μm for A and B, 500 μm for C and D.

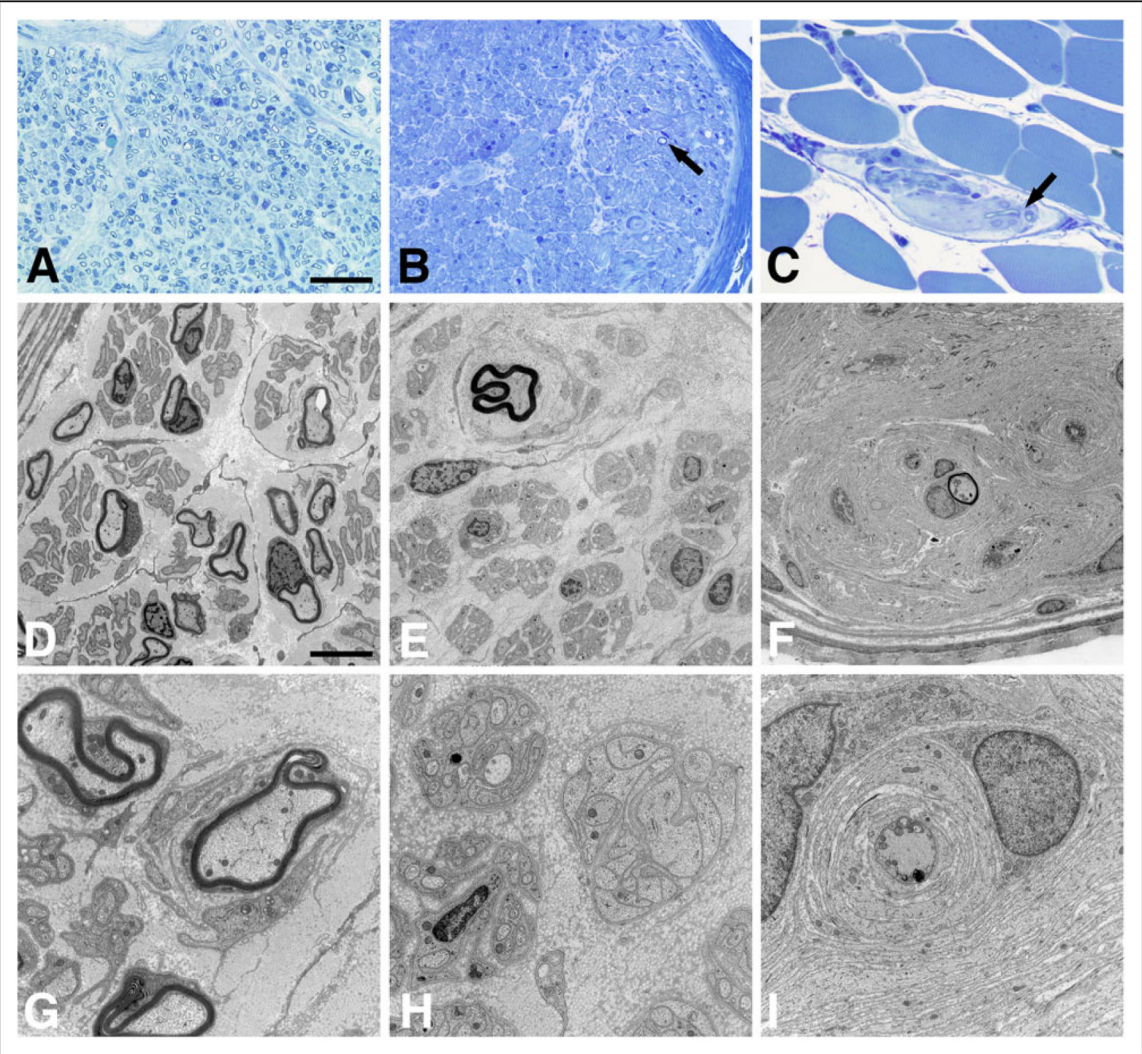


Figure 3. Nerve biopsy pathology in *CNTNAP1* mutated individuals. Panels show peripheral nerve pathology in the sural nerve at 1 month (A, D, and G), sural nerve at 3.5 years (B, E, and H), and intramuscular nerve twigs at 3.5 years (C, F, and J). There is a striking progression of myelinated axon loss between 1 month and 3.5 years (A and B/C, respectively; epon sections stained with toluidine blue). The arrows in panels B and C point to two of the very few myelinated axons still present at 3.5 years. Electron micrographs emphasize the paucity of myelinated axons at 3.5 years (E and F) and show onion bulb formation at 1 month (upper right corner of panel D) and 3.5 years (upper left corner of panel E; throughout panel F). Panels G and I show onion bulbs at higher magnification. The axon in the middle of the onion bulb in panel I has features of dystrophic pathology. The upper right corner of panel H shows a large band of Bungner (cluster of Schwann cell processes without an axon). The size bar in panel A is 50 μm for A, B, and C. The size bar in panel D is 15 μm for D, E, and F, and the size bar in panel G is 5 μm for G, H, and I.

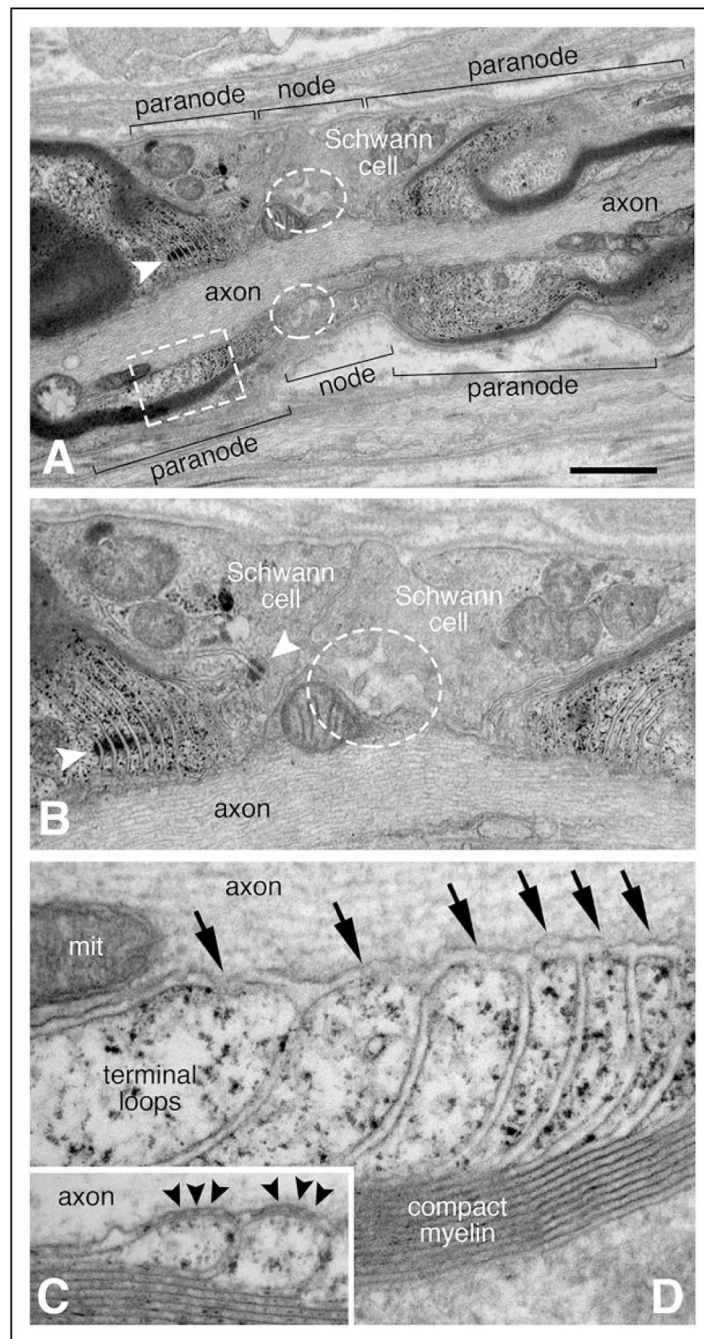


Figure 4. Abnormal node of Ranvier ultrastructure. Panels A, B, and D are from a single node of Ranvier observed in the sural nerve biopsy performed at 3.5 years of age; panel C is from a control adult sural nerve. The approximate borders for the node and the paranodal regions are delimited by brackets (A). Instead of normal microvilli, broad Schwann cell processes extend into the nodal region from either side (A and B). Only a small number of blunted microvilli are present at the node (white dashed line ovals in A and B). Normal appearing adherens junctions are noted between adjacent, uniform terminal loops of the left heminode

(white arrowhead in A; left white arrowhead in B). The adherens junction nearest the node (right white arrowhead in B) marks the boundary of several abnormally shaped terminal loops. Many of the terminal loops (marked by the white dashed line rectangle in panel A and shown at higher magnification in D) appear to arise normally from compact myelin. However, the septate axoglial paranodal junctions that normally bridge between the tip of each terminal loop to the axolemma (black arrowheads in C) are absent from the patient (arrows in D). The size bar in panel A equals 1.2 μm in panel A, 0.6 μm in panel B, and 0.15 μm in panels C and D. The structure in the axoplasm of panel D labeled “mit” is a mitochondrion.